Distributed Collaborative Control of Redundant Robots Under Weight-Unbalanced Directed Graphs

Xin Zheng, Mei Liu, Long Jin, *Senior Member, IEEE*, and Chenguang Yang, *Senior Member, IEEE*

***Abstract*—In consideration of the limitation of the communication and the possibility that redundant robots might deliver information at different power levels, cases under weight-unbalanced directed graphs from the network topology perspective are in larger accordance with those in multiple redundant robot systems. By moving forward along this direction, a distributed controller is proposed in this paper to handle circumstances of collaborative control of multiple redundant robots under weight-unbalanced directed graphs. This kind of control problem is modelled into generalized quadratic programming (QP) problems with equality and inequality constraints. Then, the above QP problems are solved by a proposed neural-dynamics-based method, whose stability and convergence are theoretically proved subsequently. Besides, several experimental examples are conducted, and related comparisons are provided to demonstrate the feasibility of the proposed controller.**

***Index Terms*—Distributed collaborative control, weight-unbalanced directed graph, neural dynamics, redundant robot.**

I. Introduction

WITH the development of industrial automation and computer technology, robotics begins to enter the stage of large-scale production and practical application [1]–[4]. Unlike non-redundant robots, redundant robots possess extra degrees of freedom (DOFs) and thus enjoy more flexibility to handle complicated tasks with better performance. The research on the control of a redundant robot has obtained considerable achievements [5]–[9]. In [5], the kinematic control of a single redundant manipulator with physical constraints is analyzed by a recursive recurrent neural network-based model. The kinematic control of a single redundant robot is analyzed for tracking a moving object with obstacles involved [6]. Xie *et al.* present a data-driven scheme with a neural dynamics solver involved in [9] to accurately estimate the Jacobian matrix and realize the kinematic control of a model-unknown robot.

This work was supported in part by the National Natural Science Foundation of China under Grant 62176109 and Grant 62311530099, in part by the Natural Science Foundation of Gansu Province under Grant 21JR7RA531 and Grant 22JR5RA487, in part by the CAAI-Huawei MindSpore Open Fund under Grant CAAIXSJLJJ-2022-020A, in part by the Industry-University-Research Innovation Fund for Chinese Universities under Grant 2021ZYA05002, in part by the Natural Science Foundation of Sichuan Province under Grant 2022nsfsc0916, in part by the Joint Education Project of Universities in China-Central and Eastern European Countries under Grant 2022226, in part by the Fundamental Research Funds for the Central Universities under Grant lzujbky-2022-23, and in part by the Supercomputing Center of Lanzhou University. (*Xin Zheng and Mei Liu are co-first authors.*) (*Corresponding author: Long Jin.*)

Xin Zheng, Mei Liu, and Long Jin are with the School of Information Science and Engineering, Lanzhou University, Lanzhou 730000, China (e-mails: xzheng20@lzu.edu.cn; mliu@lzu.edu.cn; jinlongsysu@foxmail.com). Chenguang Yang is with the Bristol Robotics Laboratory, University of the West of England, BS16 1QY Bristol, U.K. (e-mail: cyang@ieee.org).

Due to the high demand in both social and industrial communities, one single redundant robot nowadays is labored to cope with complex tasks which are large-scale and overloaded. Therefore, two or more redundant robots are introduced to complete given complicated missions collaboratively. For instance, in the recent automobile industry, multiple redundant robots are utilized for coordinated welding [10], which can be seen as the collaborative control of redundant robots. Besides, in the clinical medicine field, the robot-assisted surgery [11], which requires multiple redundant robots to complete an operation collaboratively with high accuracy, can also be seen as a promising application scenario. As a result, the research on the collaborative control of multiple redundant robot systems (MR^2S) has been flourishing in the past decades with different contributions. Gueaieb *et al.* present a decentralized adaptive hybrid intelligent scheme in [12] for the position synchronizing and force control in MR^2S. A decentralized kinematic controller for the collaborative control of MR^2S is investigated in [13]. Then, in [14], the energy and manipulability of multiple mobile robots are optimized for their distributed cooperative transportation control. Ge *et al.* design a unified framework and a scalable platooning control method for the distributed cooperative control of multiple movable robots [15]. A method containing both holonomic and nonholonomic structures is introduced in [16] for the tracking control of multiple mobile robots with disturbances. Besides, impedance learning is applied in a fuzzy neural network for carrying objects in MR^2S [17], and a summary of the latest outcomes of coordinated control of multiple autonomous surface vehicles are introduced in [18].

Neural-dynamics-based controllers in MR^2S have been developed in the past few years and have obtained satisfying results. Neural dynamics, which is deemed a powerful strategy to deal with complex problems, has attracted more and more attention from researchers around the world, with various high-level outcomes published consequently [19]–[22]. For instance, in [21], a neural dynamics method with variant gain is presented and applied for handling time-variant matrix formulas. In general, neural dynamics methods own better performance than traditional ones [23] when conducting high nonlinear tasks because of their outstanding computational power and low consumption, which can be applied as an effective algorithm for the motion planning of redundant robots that is established in the form of an ordinary differential equation. Therefore, it would be a rational decision to utilize neural dynamics methods for controlling MR^2S. For example, reference [24] puts forward a neural-dynamics-based distributed cooperative control scheme for MR^2S to

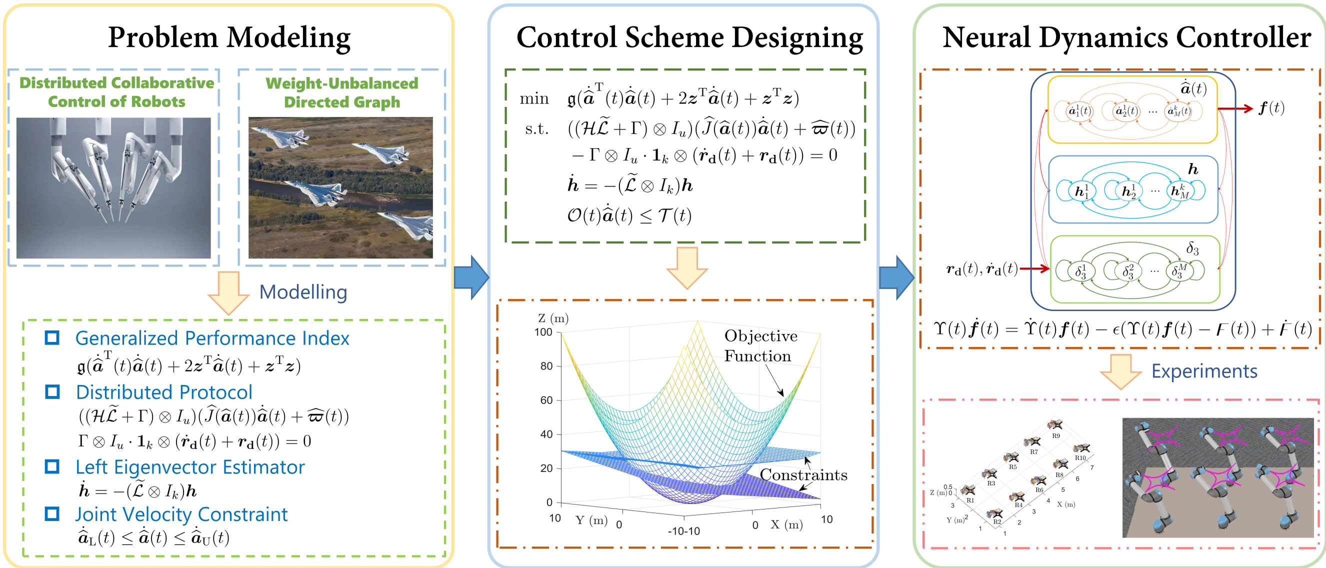

Fig. 1. The research route of this paper.

improve communication efficiency from a game-theoretical perspective. An optimization model and its associated solver based on neural dynamics are constructed for the distributed and delay-considered collaborative control of MR^2S [25]. Yet, it can be found that previous published papers related to the distributed collaborative control of MR^2S only focus on undirected or weight-balanced directed topologies, which is not applicable for the common realistic scenarios whose topologies are weight-unbalanced directed. In order to solve this problem, we propose a distributed and weight-unbalanced neural dynamics controller for MR^2S based on the graph theory for the first time.

Graph theory, which can be used to describe the topology of a network, is seen as one of the significant fundamentals of MR^2S and under wide discussions nowadays. It is worth mentioning that circumstances under weight-unbalanced directed graphs are very common in both industrial and social domains, especially in a distributed network. For example, in the latest Russia-Ukraine conflict, the air force of Russia dispatches four Sukhoi Su-57 for target-tracking missions. They adopt a distributed information network to decrease the detection from the target's radars [26], in which only one Sukhoi Su-57 opens the radar and then transfers the obtained coordinate of the target to others in a distributed manner. It can be seen that the topology among the target and four Sukhoi Su-57 is weight-unbalanced. Besides, there often exists a situation where an agent i can be aware of another agent j but not vice versa because of the restricted field of vision. Additionally, different agents are likely to utilize devices that possess different propagation power levels when communicating with other agents. Furthermore, if the stability and convergence of a proposed scheme are still guaranteed after an original ideal weight-balanced directed graph transfers to be weight-unbalanced, this scheme is evidently more trusted. Therefore, considering circumstances under weight-unbalanced directed graphs when analyzing the distributed collaborative control of MR^2S is necessary and beneficial. Actually, there have been a few high-quality results related to the weight-unbalanced directed graph in recent years [27]–[30]. In [28], a constrained convex optimization problem is solved by a distributed randomized protocol of multi-agent systems under weight-unbalanced directed graphs. Two algorithms are designed in [29] for investigating the distributed average tracking problems under weight-unbalanced directed graphs. However, existing results under weight-unbalanced directed graphs are based on multi-agent systems that are developed at the particle level, and none of them introduces circumstances under weight-unbalanced directed graphs into the collaborative control of MR^2S with robot kinematics contained. As such, those previous outcomes are not able to be utilized to handle the collaborative control under weight-unbalanced directed graphs in MR^2S. In this paper, a distributed scheme and an associated neural dynamics controller are firstly proposed to handle the above circumstances.

In this work, the authors propose a neural dynamics-based controller for the collaborative control of MR^2S under weight-unbalanced directed graphs. Fig. 1 displays the research route for briefly introducing this paper. In detail, this control system can be modelled and constructed as a quadratic programming (QP) optimization problem, in which a generalized performance index is set as the objective function. Then, a neural dynamics controller is designed to solve it online with theoretical analyses conducted subsequently. Additionally, the effectiveness of the proposed neural dynamics controller is validated by several simulative examples and comparisons. Specifically, there are two essential challenges about handling weight-unbalanced directed graphs in the investigation process of this paper. The first challenge is how to integrate weight-unbalanced directed graphs into the control scheme of the distributed collaborative control of MR^2Ss, and the second one is how to analyze the stability and convergence of the proposed scheme rigorously with practical redundant robots considered. These challenges are solved in Section II and Section III. In sum, the main contributions of this work are listed as follows:

1) It investigates the distributed collaborative control of MR^{2}S under circumstances of weight-unbalanced directed graphs for the first time with robot kinematics contained.
2) It models the distributed collaborative control of MR^{2}S as a generalized QP optimization problem with equality and inequality constraints, and an estimator for the required left eigenvector is introduced. Then, the above QP problem is solved by a proposed neural-dynamics-based method, whose stability and convergence are theoretically proved.

There are four sections being provided for the rest of this work. In detail, Section II models an optimization problem for the distributed collaborative control of MR^{2}S under weight-unbalanced directed graphs. In Section III, the corresponding neural dynamics controller and related theoretical analyses are designed and proved. Then, Section IV analyzes several simulative examples and offers comparisons to verify the validity of the proposed distributed controller. At last, Section V concludes the whole paper.

II. Preliminaries

This section offers preliminaries of the graph theory and redundant robots. Then, a distributed collaborative controller of MR^{2}S under weight-unbalanced directed graphs is modelled as a convex optimization problem. Before introducing preliminaries, Table I provides explanations of important symbols in this paper.

TABLE I
Explanations of Important Symbols in This Paper

$\widetilde{\mathcal{N}}_i$	The set of in-neighbors of robot i in which $\widetilde{\mathcal{N}}_0$ represents the robots that are accessed to the information of the command center
k	The number of robots
T	The transpose of a vector or a matrix
$\boldsymbol{\varpi}_i(t) \in \mathbb{R}^u$	$\boldsymbol{\varpi}_i(t)$ denotes the actual path of the robot i's end-effector
$\widehat{\boldsymbol{\varpi}}(t) \in \mathbb{R}^{uk}$	$\widehat{\boldsymbol{\varpi}}(t) = \left[\boldsymbol{\varpi}_1^{\mathrm{T}}(t), \cdots, \boldsymbol{\varpi}_k^{\mathrm{T}}(t)\right]^{\mathrm{T}}$
ζ_i	parameter ζ_i is used for reflecting the accessing relationship between robot i and the command center, i.e., $i \in \widetilde{\mathcal{N}}_0 \to \zeta_i = 1$ and $i \notin \widetilde{\mathcal{N}}_0 \to \zeta_i = 0$
$\Gamma \in \mathbb{R}^{k\times k}$	A diagonal matrix whose diagonal element is ζ_i
$\otimes$	The Kronecker product
$\boldsymbol{h}_i \in \mathbb{R}^k$	The estimate of the left eigenvector of robot i when the eigenvalue of $\widetilde{\mathcal{L}}$ equals 0, and h_{ii} is the ith element of $\boldsymbol{h}_i$
$\mathcal{H} \in \mathbb{R}^{k\times k}$	$\mathcal{H} = \mathrm{diag}([h_{11}, h_{22}, \cdots, h_{kk}])$
$\boldsymbol{h} \in \mathbb{R}^{k^2}$	$\boldsymbol{h} = [\boldsymbol{h}_1^{\mathrm{T}}, \cdots, \boldsymbol{h}_k^{\mathrm{T}}]^{\mathrm{T}}$
$\mathbf{1}_k \in \mathbb{R}^k$	A vector composed by k elements 1
$I_u \in \mathbb{R}^{u\times u}$	An identity matrix with order u
$\widetilde{\mathcal{L}} \in \mathbb{R}^{k\times k}$	The Laplacian matrix
$\widehat{\boldsymbol{a}}(t) \in \mathbb{R}^{mk}$	$\widehat{\boldsymbol{a}}(t) = \left[\boldsymbol{a}_1^{\mathrm{T}}(t), \cdots, \boldsymbol{a}_k^{\mathrm{T}}(t)\right]^{\mathrm{T}}$

A. Graph Theory

Define $\widetilde{\mathcal{G}} = (\widetilde{\mathcal{V}}, \widetilde{\mathcal{E}}, \widetilde{\mathcal{W}})$ as a weighted-unbalanced digraph with $\widetilde{\mathcal{V}} = \{1, \cdots, k\}$ the set of nodes and $\widetilde{\mathcal{E}} \subseteq \widetilde{\mathcal{V}} \times \widetilde{\mathcal{V}}$ the set of edges. For example, if (j,i) is an edge, the node j can deliver its information to node i. $\widetilde{\mathcal{W}} = [w_{ij}] \in \mathbb{R}^{k\times k}$ denotes the weighted adjacency matrix with $w_{ij} \in \{0, \bar{w}\}, w_{ij} = \bar{w} \in \mathbb{R}^+$, if $(j,i) \in \widetilde{\mathcal{E}}$ and $w_{ij} = 0$ otherwise. Let $\widetilde{\mathcal{N}}_i = \{j \in \widetilde{\mathcal{V}} : (j,i) \in \widetilde{\mathcal{E}}\}$ denote the set of in-neighbors of node i. A directed path is a sequence of nodes connected by edges. A digraph is strongly connected if for every pair of nodes there is a directed path connecting them. The k-dimensional square Laplacian matrix $\widetilde{\mathcal{L}}$ is composed of $[l_{ij}]$, which is defined as $l_{ii} = \sum_{j=1, j\neq i}^{k} w_{ij}$ and $l_{ij} = -w_{ij}$, where $i \neq j$. It can be seen that $\widetilde{\mathcal{L}}\mathbf{1}_k = \mathbf{0}_k$. A directed graph is weight-balanced if and only if $\mathbf{1}_k^{\mathrm{T}}\widetilde{\mathcal{L}} = \mathbf{0}_k^{\mathrm{T}}$, and $\sum_{j\in\widetilde{\mathcal{V}}} w_{ij} = \sum_{j\in\widetilde{\mathcal{V}}} w_{ji}$ for $i \in \widetilde{\mathcal{V}}$. A left eigenvector $\boldsymbol{p}^{\mathrm{T}} = [\boldsymbol{p}_1, \cdots, \boldsymbol{p}_k]$ corresponding to an eigenvalue λ of $\widetilde{\mathcal{L}}$ means that $\boldsymbol{p}^{\mathrm{T}}\widetilde{\mathcal{L}} = \lambda\boldsymbol{p}^{\mathrm{T}}$. Then, we have the following Lemma.

Lemma 1: [31] [32] The strong-connect digraph $\widetilde{\mathcal{G}} = (\widetilde{\mathcal{V}}, \widetilde{\mathcal{E}}, \widetilde{\mathcal{W}})$ with its Laplacian matrix $\widetilde{\mathcal{L}} = [l_{ij}] \in \mathbb{R}^{k\times k}$ meets the following items.

1) Its Laplacian matrix $\widetilde{\mathcal{L}}$ possess a left eigenvector $\boldsymbol{q}^{\mathrm{T}} = [\boldsymbol{q}_1, \cdots, \boldsymbol{q}_k]$ corresponding to the eigenvalue 0, which satisfies that $\boldsymbol{q}_i > 0, i = 1, \cdots, k, \boldsymbol{q}^{\mathrm{T}}\widetilde{\mathcal{L}} = \mathbf{0}_k^{\mathrm{T}}$, and $\sum_{i=1}^{k} \boldsymbol{q}_i = 1$.
2) $\min_{\beta^{\mathrm{T}}\boldsymbol{b}=0, \boldsymbol{b}\neq\mathbf{0}_k} \boldsymbol{b}^{\mathrm{T}}\hat{\mathcal{L}}\boldsymbol{b} > \lambda_2(\hat{\mathcal{L}})\boldsymbol{b}^{\mathrm{T}}\boldsymbol{b}/k$, in which $\beta > 0$ and $\boldsymbol{b}$ are arbitrary vectors, $\hat{\mathcal{L}} = \widetilde{\mathcal{L}}^{\mathrm{T}}\,\widetilde{\mathcal{Q}} + \widetilde{\mathcal{Q}}\widetilde{\mathcal{L}}$ with $\widetilde{\mathcal{Q}} = \mathrm{diag}(\boldsymbol{q}) \in \mathbb{R}^{k\times k}$, and $\lambda_2(\hat{\mathcal{L}})$ denotes the second smallest eigenvalue of $\hat{\mathcal{L}}$.
3) $\lim_{t\to\infty} \exp(-\widetilde{\mathcal{L}}t) = \mathbf{1}_k\boldsymbol{q}^{\mathrm{T}}$.

B. Forward Kinematics

As for an m-DOF redundant robot i, whose joint angles can be expressed in a vector-form $\boldsymbol{a}_i(t) = \left[\boldsymbol{a}_{i1}(t), \boldsymbol{a}_{i2}(t), \cdots, \boldsymbol{a}_{im}(t)\right]^{\mathrm{T}} \in \mathbb{R}^m$. Besides, robot i's u-dimensional coordinate in the work space $\boldsymbol{r}_i(t) \in \mathbb{R}^u$ can be acquired by $\boldsymbol{r}_i(t) = \varPhi(\boldsymbol{a}_i(t))$, in which $\varPhi(\cdot)$ can be seen as a mapping operation. Specifically, robot i's desired path is denoted as $\boldsymbol{r}_{\mathbf{d}i}(t) \in \mathbb{R}^u$ in the following with $\boldsymbol{r}_{\mathbf{d}}(t)$ representing that of the command center, and m is supposed to be larger than u according to the redundant properties. Then, differentiating both sides of the above equation, we can obtain that $\dot{\boldsymbol{r}}_i(t) = J(\boldsymbol{a}_i(t))\,\dot{\boldsymbol{a}}_i(t)$, where $J(\boldsymbol{a}_i(t)) = \mathrm{d}\varPhi(\boldsymbol{a}_i(t))/\mathrm{d}\boldsymbol{a}_i(t) \in \mathbb{R}^{u\times m}$ represents the Jacobian matrix.

C. Problem Modelling

In this section, a distributed collaborative controller of MR^{2}S under weight-unbalanced directed graphs is proposed. Assuming a system composed of k redundant robots, its interaction topology can be depicted by a weight-unbalanced directed graph $\widetilde{\mathcal{G}}$.

Assumption 1: $\widetilde{\mathcal{G}}$ is invariable and strongly connected.

In real-world scenarios, the suitable left eigenvector $\boldsymbol{q}^{\mathrm{T}}$ associated with the zero eigenvalue of the Laplacian matrix $\widetilde{\mathcal{L}}$ is quite hard to obtain, especially for large-scale MR^{2}S. Therefore, in order to analyze the above control problem under weight-unbalanced directed graphs, an estimator $\boldsymbol{h}(t)$ of $\boldsymbol{q}$ is designed as follows:

$$\dot{\boldsymbol{h}}_i(t) = -\sum_{j\in\widetilde{\mathcal{N}}_i} w_{ij}(\boldsymbol{h}_i(t) - \boldsymbol{h}_j(t)), \quad (1)$$

where $\boldsymbol{h}_i(t), \boldsymbol{h}_j(t) \in \mathbb{R}^k$ denote the estimates of the left eigenvector of robot i and robot j when the eigenvalue of $\widetilde{\mathcal{L}}$ equals 0, respectively.

Besides, all k redundant robots are connected in a distributed manner, which means that a robot i can only receive information from the robots in its set of in-neighbors, e.g. $\widetilde{\mathcal{N}}_i$, in which $\widetilde{\mathcal{N}}_0$ represents the robots that are accessed to the information of the command center, which means that the signal from the command center can only transfer to robots whose set of in-neighbors contains it in other words. Then, we formulate a distributed equation for robot i with estimator (1) associated for realizing the above distributed behaviors:

$$\begin{aligned} &h_{ii}(t)\sum_{j\in\widetilde{\mathcal{N}}_i}\{w_{ij}[\dot{\boldsymbol{\varpi}}_i(t) - \dot{\boldsymbol{\varpi}}_j(t) + \boldsymbol{\varpi}_i(t) - \boldsymbol{\varpi}_j(t)] \\ &+\zeta_i[\dot{\boldsymbol{\varpi}}_i(t) - \dot{\boldsymbol{r}}_{\mathbf{d}}(t) + \boldsymbol{\varpi}_i(t) - \boldsymbol{r}_{\mathbf{d}}(t)]\} = \mathbf{0}, \\ &\dot{\boldsymbol{h}}_i(t) = -\sum_{j\in\widetilde{\mathcal{N}}_i} w_{ij}(\boldsymbol{h}_i(t) - \boldsymbol{h}_j(t)), \end{aligned} \quad (2)$$

where $h_{ii}(t)$ is the ith element of $\boldsymbol{h}_i(t)$, $h_{ii}(0) = 1$ when $i \in \widetilde{\mathcal{V}}$, and $h_{ij}(0) = 0$ when $i \neq j$; w_{ij} is a connection weight between robot i and robot j; $\boldsymbol{\varpi}_i(t) \in \mathbb{R}^u$ denotes the actual path of the robot i's end-effector; parameter ζ_i is used for reflecting the accessing relationship between robot i and the command center, i.e., $i \in \widetilde{\mathcal{N}}_0 \to \zeta_i = 1$ and $i \notin \widetilde{\mathcal{N}}_0 \to \zeta_i = 0$; $\dot{\boldsymbol{r}}_{\mathbf{d}}(t)$ represents the desired velocity of the end-effector of a robot. Compact forms of (2) for all robots are

$$\begin{aligned} &(\mathcal{H}\widetilde{\mathcal{L}} \otimes I_u)(\dot{\widehat{\boldsymbol{\varpi}}}(t) + \widehat{\boldsymbol{\varpi}}(t)) + (\Gamma \otimes I_u)(\dot{\widehat{\boldsymbol{\varpi}}}(t) \\ &+ \widehat{\boldsymbol{\varpi}}(t)) - \mathbf{1}_k \otimes (\dot{\boldsymbol{r}}_{\mathbf{d}}(t) + \boldsymbol{r}_{\mathbf{d}}(t)) = \mathbf{0}, \\ &\dot{\boldsymbol{h}}(t) = -(\widetilde{\mathcal{L}} \otimes I_k)\boldsymbol{h}(t), \end{aligned} \quad (3)$$

where $\mathcal{H} = \mathrm{diag}([h_{11}, h_{22}, \cdots, h_{kk}])$ is a k-dimensional matrix; $\boldsymbol{h}(t) = [\boldsymbol{h}_1(t)^{\mathrm{T}}, \boldsymbol{h}_2(t)^{\mathrm{T}}, \cdots, \boldsymbol{h}_k(t)^{\mathrm{T}}]^{\mathrm{T}} \in \mathbb{R}^{k^2}$; $\widehat{\boldsymbol{\varpi}}(t) = \left[\boldsymbol{\varpi}_1^{\mathrm{T}}(t), \cdots, \boldsymbol{\varpi}_k^{\mathrm{T}}(t)\right]^{\mathrm{T}} \in \mathbb{R}^{uk}$; $\dot{\widehat{\boldsymbol{\varpi}}}(t) = \left[\dot{\boldsymbol{\varpi}}_1^{\mathrm{T}}(t), \cdots, \dot{\boldsymbol{\varpi}}_k^{\mathrm{T}}(t)\right]^{\mathrm{T}} \in \mathbb{R}^{uk}$; $\Gamma = \mathrm{diag}([\zeta_1, \zeta_2, \cdots, \zeta_k]) \in \mathbb{R}^{k\times k}$; I_u and I_k represent two identity matrices with their dimensions being $u\times u$ and $k\times k$, respectively. Specifically, $\mathcal{H}\mathcal{L}$ means the equivalent Laplacian matrix of the weight-balanced directed graph. Then, deducing from the forward kinematics, we can obtain two equality constraints by substituting $\dot{\widehat{\boldsymbol{\varpi}}}(t)$ to $\widehat{J}(\widehat{\boldsymbol{a}}(t))\dot{\widehat{\boldsymbol{a}}}(t)$:

$$\begin{aligned} &((\mathcal{H}\widetilde{\mathcal{L}} + \Gamma) \otimes I_u)(\widehat{J}(\widehat{\boldsymbol{a}}(t))\dot{\widehat{\boldsymbol{a}}}(t) + \widehat{\boldsymbol{\varpi}}(t)) \\ &- \Gamma \otimes I_u \cdot \mathbf{1}_k \otimes (\dot{\boldsymbol{r}}_{\mathbf{d}}(t) + \boldsymbol{r}_{\mathbf{d}}(t)) = \mathbf{0}, \\ &\dot{\boldsymbol{h}}(t) = -(\widetilde{\mathcal{L}} \otimes I_k)\boldsymbol{h}(t), \end{aligned} \quad (4)$$

where

$$\widehat{J}(\widehat{\boldsymbol{a}}(t)) = \begin{bmatrix} J_1(\boldsymbol{a}_1(t)) & 0 & \cdots & 0 \\ 0 & J_2(\boldsymbol{a}_2(t)) & \cdots & 0 \\ \vdots & \vdots & \ddots & \vdots \\ 0 & 0 & \cdots & J_k(\boldsymbol{a}_k(t)) \end{bmatrix} \in \mathbb{R}^{uk\times mk},$$

with $J_i(\boldsymbol{a}_i(t)) \in \mathbb{R}^{u\times m}$ standing for the Jacobian matrix of robot i; $\widehat{\boldsymbol{a}}(t) = \left[\boldsymbol{a}_1^{\mathrm{T}}(t), \cdots, \boldsymbol{a}_k^{\mathrm{T}}(t)\right]^{\mathrm{T}}$.

Furthermore, in order to limit the velocities of end-effectors, an inequality constraint is introduced as follows:

$$\dot{\widehat{\boldsymbol{a}}}_{\mathrm{L}}(t) \le \dot{\widehat{\boldsymbol{a}}}(t) \le \dot{\widehat{\boldsymbol{a}}}_{\mathrm{U}}(t), \quad (5)$$

in which $\dot{\widehat{\boldsymbol{a}}}_{\mathrm{L}}(t)$ and $\dot{\widehat{\boldsymbol{a}}}_{\mathrm{U}}(t)$ denote the lower bound and the upper bound of $\widehat{\boldsymbol{a}}(t)$, respectively. Then, this inequality constraint can be reconstructed as $\mathcal{O}(t)\dot{\widehat{\boldsymbol{a}}}(t) \le \mathcal{T}(t)$, where $\mathcal{O}(t) = [-I_{mk}, I_{mk}]^{\mathrm{T}}$, $\mathcal{T}(t) = [-\dot{\widehat{\boldsymbol{a}}}_{\mathrm{L}}^{\mathrm{T}}(t), \dot{\widehat{\boldsymbol{a}}}_{\mathrm{U}}^{\mathrm{T}}(t)]^{\mathrm{T}}$.

Before continuing to design the available scheme, the convergence of the formulated equality constraints (3) is required to be proved. According to the distributed protocol presented in (2), it can be seen that the desired path $\boldsymbol{r}_{\mathbf{d}}(t)$ and its time derivative $\dot{\boldsymbol{r}}_{\mathbf{d}}(t)$ only deliver to robots whose serial numbers exist in $\widetilde{\mathcal{N}}_0$. Besides, the correctness of the estimator (1) also needs to be verified to reflect the effectiveness of equality constraints. Based on Assumption 1, Theorem 1 below offers proofs to verify that equality constraints in (4) have the same impact with $\boldsymbol{\varpi}_i(t) = \boldsymbol{r}_{\mathbf{d}}(t)$, $\dot{\boldsymbol{\varpi}}_i(t) = \dot{\boldsymbol{r}}_{\mathbf{d}}(t)$, and $\lim_{t\to\infty} \mathcal{H} \to \widetilde{\mathcal{Q}}$.

Theorem 1: MR^{2}S equipped with the distributed consensus filter is modelled in (3), of each robot has the desired trajectory and joint velocities when Assumption 1 maintains, i.e., $\boldsymbol{\varpi}_i(t) = \boldsymbol{r}_{\mathbf{d}}(t)$ and $\dot{\boldsymbol{\varpi}}_i(t) = \dot{\boldsymbol{r}}_{\mathbf{d}}(t)$. Besides, the estimator for the equivalent Laplacian matrix of the weight-balanced directed graph in (3) is effective, i.e., $\lim_{t\to\infty} \mathcal{H} \to \widetilde{\mathcal{Q}}$.

Proof: From the first formula of (3), one can deduce that

$$\begin{aligned} &((\mathcal{H}\widetilde{\mathcal{L}} + \Gamma) \otimes I_u)(\dot{\widehat{\boldsymbol{\varpi}}}(t) + \widehat{\boldsymbol{\varpi}}(t)) \\ &-\Gamma \otimes I_u \cdot \mathbf{1}_k \otimes (\dot{\boldsymbol{r}}_{\mathbf{d}}(t) + \boldsymbol{r}_{\mathbf{d}}(t)) = \mathbf{0}. \end{aligned} \quad (6)$$

A matrix $\mathcal{M}$ is designed as follows:

$$\mathcal{M} = \begin{bmatrix} \mathcal{H}\widetilde{\mathcal{L}} + \Gamma & -\Gamma \\ -\Gamma & \Gamma \end{bmatrix} \in \mathbb{R}^{2k\times 2k}.$$

Then, (6) can be rewritten to

$$(\mathcal{M} \otimes I_u)\dot{\check{\boldsymbol{\varpi}}}(t) = \mathbf{0}, \quad (7)$$

where $\dot{\check{\boldsymbol{\varpi}}}(t) = [\dot{\widehat{\boldsymbol{\varpi}}}(t) + \widehat{\boldsymbol{\varpi}}(t), \mathbf{1}_k \otimes (\dot{\boldsymbol{r}}_{\mathbf{d}}(t) + \boldsymbol{r}_{\mathbf{d}}(t))]$. As Assumption 1 mentions, the graph is strongly connected, so we can obtain that the singular matrix $\mathcal{M}$ involves a null space for the vector $\mathbf{1}_{2k}$. Afterwards, equation (7) is evidently consistent with $\dot{\check{\boldsymbol{\varpi}}}(t) = \mathbf{1}_{2k} \otimes (\dot{\boldsymbol{\varpi}}'(t) + \boldsymbol{\varpi}'(t)) = [(\dot{\boldsymbol{\varpi}}'(t) + \boldsymbol{\varpi}'(t))^{\mathrm{T}}, (\dot{\boldsymbol{\varpi}}'(t) + \boldsymbol{\varpi}'(t))^{\mathrm{T}}, \cdots, (\dot{\boldsymbol{\varpi}}'(t) + \boldsymbol{\varpi}'(t))^{\mathrm{T}}]$. Further, as we compare the above equation with $\dot{\check{\boldsymbol{\varpi}}}(t) = [\dot{\widehat{\boldsymbol{\varpi}}}(t) + \widehat{\boldsymbol{\varpi}}(t), \mathbf{1}_k \otimes (\dot{\boldsymbol{r}}_{\mathbf{d}}(t) + \boldsymbol{r}_{\mathbf{d}}(t))]$, we can readily obtain a conclusion that $\dot{\boldsymbol{r}}_{\mathbf{d}}(t) + \boldsymbol{r}_{\mathbf{d}}(t) = \dot{\boldsymbol{\varpi}}_1(t) + \boldsymbol{\varpi}_1(t) = \dot{\boldsymbol{\varpi}}_2(t) + \boldsymbol{\varpi}_2(t) = \cdots = \dot{\boldsymbol{\varpi}}_k(t) + \boldsymbol{\varpi}_k(t)$. Therefore, when Assumption 1 maintains and MR^{2}S come to the steady state, $\boldsymbol{\varpi}_i(t) = \boldsymbol{r}_{\mathbf{d}}(t)$ and $\dot{\boldsymbol{\varpi}}_i(t) = \dot{\boldsymbol{r}}_{\mathbf{d}}(t)$ are satisfied.

Besides, it can be seen that $\boldsymbol{h}(t)=\exp((-\widetilde{\mathcal{L}}\otimes I_u)t)\boldsymbol{h}(0)$. Then, according to Lemma 1, one can get that $\lim_{t\to\infty}\boldsymbol{h}(t)=\exp(\mathbf{1}_k\boldsymbol{q}^{\mathrm{T}}\otimes I_k)\boldsymbol{h}(0)=\mathbf{1}_k\otimes\boldsymbol{q}$. Therefore, $\lim_{t\to\infty}\mathcal{H}\to\widetilde{\mathcal{Q}}$ is proved as well when Assumption 1 maintains. ■

It can be obtained from Lemma 1 that $\mathcal{H}$ is able to estimate $\widetilde{\mathcal{Q}}$, and it is known that $\mathbf{1}_k^{\mathrm{T}}\widetilde{\mathcal{Q}}\widetilde{\mathcal{L}}=\mathbf{0}_k^{\mathrm{T}}$, which means that the equivalent Laplacian matrix of the weight-balanced directed graph can be calculated by the estimator (1) successfully [33]. In sum, the convergence of distributed equality constraints (3) is theoretically guaranteed.

D. Distributed Scheme Design

Redundant robots have the nature of redundancy, which means that there may exist not only one solution conforming to (4). Therefore, an available performance index is required as the objective function of the optimization problem. In this paper, we adopt a generalized performance index $\mathcal{A}$ to increase the scalability of our proposed scheme:

$$\begin{aligned}\mathcal{A}&=\Psi(\hat{\boldsymbol{a}}(t))\\&=\mathfrak{g}\|\dot{\hat{\boldsymbol{a}}}(t)+\boldsymbol{z}\|_2^2\\&=\mathfrak{g}(\dot{\hat{\boldsymbol{a}}}^{\mathrm{T}}(t)\dot{\hat{\boldsymbol{a}}}(t)+2\boldsymbol{z}^{\mathrm{T}}\dot{\hat{\boldsymbol{a}}}(t)+\boldsymbol{z}^{\mathrm{T}}\boldsymbol{z}),\end{aligned}\tag{8}$$

where $\mathfrak{g}>0$; $\boldsymbol{z}\in\mathbb{R}^{mk}$ represents a criterion, such as joint drift and manipulability.

Afterwards, a QP optimization problem can be modelled by combing the objective function and constraints:

$$\begin{aligned}\min\quad&\mathfrak{g}(\dot{\hat{\boldsymbol{a}}}^{\mathrm{T}}(t)\dot{\hat{\boldsymbol{a}}}(t)+2\boldsymbol{z}^{\mathrm{T}}\dot{\hat{\boldsymbol{a}}}(t)+\boldsymbol{z}^{\mathrm{T}}\boldsymbol{z}),\\ \text{s.t.}\quad&((\mathcal{H}\widetilde{\mathcal{L}}+\Gamma)\otimes I_u)(\widehat{J}(\hat{\boldsymbol{a}}(t))\dot{\hat{\boldsymbol{a}}}(t)+\widehat{\boldsymbol{\varpi}}(t))\\&-\Gamma\otimes I_u\cdot\mathbf{1}_k\otimes(\dot{\boldsymbol{r}}_{\mathbf{d}}(t)+\boldsymbol{r}_{\mathbf{d}}(t))=\mathbf{0},\\&\dot{\boldsymbol{h}}(t)=-(\widetilde{\mathcal{L}}\otimes I_k)\boldsymbol{h}(t),\\&\mathcal{O}(t)\dot{\hat{\boldsymbol{a}}}(t)\le\mathcal{T}(t),\end{aligned}\tag{9}$$

which is termed the distributed and weight-unbalanced collaborative control scheme.

III. Neural Dynamics Controller and Theoretical Analyses

In this section, a neural dynamics controller is designed for the above distributed and weight-unbalanced collaborative control scheme (9) with rigorous theoretical analyses investigated as well.

A. Neural Dynamics Controller

According to the Karush-Kuhn-Tucker conditions [34], a Lagrange function $\mathsf{LF}(\hat{\boldsymbol{a}}(t),\dot{\boldsymbol{h}}(t),\delta_1(t),\delta_2(t),\delta_3(t))$ can be obtained:

$$\begin{aligned}&\mathsf{LF}(\hat{\boldsymbol{a}}(t),\dot{\boldsymbol{h}}(t),\delta_1(t),\delta_2(t),\delta_3(t))=\mathfrak{g}\dot{\hat{\boldsymbol{a}}}^{\mathrm{T}}(t)\dot{\hat{\boldsymbol{a}}}(t)+2\mathfrak{g}\boldsymbol{z}^{\mathrm{T}}\dot{\hat{\boldsymbol{a}}}(t)\\&+\mathfrak{g}\boldsymbol{z}^{\mathrm{T}}\boldsymbol{z}+\delta_1^{\mathrm{T}}(t)(((\mathcal{H}\widetilde{\mathcal{L}}+\Gamma)\otimes I_u)(\widehat{J}(\hat{\boldsymbol{a}}(t))\dot{\hat{\boldsymbol{a}}}(t)+\widehat{\boldsymbol{\varpi}}(t))\\&-\Gamma\otimes I_u\cdot\mathbf{1}_k\otimes(\dot{\boldsymbol{r}}_{\mathbf{d}}(t)+\boldsymbol{r}_{\mathbf{d}}(t)))+\delta_2^{\mathrm{T}}(t)(\dot{\boldsymbol{h}}(t)+(\widetilde{\mathcal{L}}\otimes I_k)\boldsymbol{h}(t))\\&+\delta_3^{\mathrm{T}}(t)(\mathcal{O}(t)\dot{\hat{\boldsymbol{a}}}(t)-\mathcal{T}(t)),\end{aligned}$$

where $\delta_1(t)\in\mathbb{R}^{uk}$, $\delta_2(t)\in\mathbb{R}^{k^2}$, $\delta_3(t)\in\mathbb{R}^{2mk}$ indicate Lagrange multipliers. From [34], one can continue deducing:

$$\begin{cases}2\mathfrak{g}\dot{\hat{\boldsymbol{a}}}+2\mathfrak{g}\boldsymbol{z}+(((\mathcal{H}\widetilde{\mathcal{L}}+\Gamma)\otimes I_u)\widehat{J}(\hat{\boldsymbol{a}}(t)))^{\mathrm{T}}\delta_1(t)\\ \quad+\mathcal{O}^{\mathrm{T}}(t)\delta_3(t)=\mathbf{0},\\ I_{k^2}\delta_2(t)=\mathbf{0},\\ ((\mathcal{H}\widetilde{\mathcal{L}}+\Gamma)\otimes I_u)(\widehat{J}(\hat{\boldsymbol{a}}(t))\dot{\hat{\boldsymbol{a}}}(t)+\widehat{\boldsymbol{\varpi}}(t))\\ \quad-\Gamma\otimes I_u\cdot\mathbf{1}_k\otimes(\dot{\boldsymbol{r}}_{\mathbf{d}}(t)+\boldsymbol{r}_{\mathbf{d}}(t))=\mathbf{0},\\ \dot{\boldsymbol{h}}(t)+(\widetilde{\mathcal{L}}\otimes I_k)\boldsymbol{h}(t)=\mathbf{0},\\ \mathcal{O}(t)\dot{\hat{\boldsymbol{a}}}(t)-\mathcal{T}(t)\le 0,\delta_3(t)\ge\mathbf{0},\\ \delta_3^{\mathrm{T}}(t)(\mathcal{O}(t)\dot{\hat{\boldsymbol{a}}}(t)-\mathcal{T}(t))=\mathbf{0}.\end{cases}$$

Then, a perturbed nonlinear complementary problem function [35] is introduced to deal with the equations above:

$$\aleph_{\text{NCP}}(\boldsymbol{x},\boldsymbol{y})=\sqrt{\boldsymbol{x}\circ\boldsymbol{x}+\boldsymbol{y}\circ\boldsymbol{y}+\boldsymbol{\eta}}-\boldsymbol{x}-\boldsymbol{y},\tag{10}$$

where $\boldsymbol{\eta}\to\mathbf{0}^+$ is a perturbation term, and $\circ$ denotes the Hadamard product. Afterwards, the above equations can be rebuilt as

$$\begin{cases}2\mathfrak{g}\dot{\hat{\boldsymbol{a}}}+2\mathfrak{g}\boldsymbol{z}+(((\mathcal{H}\widetilde{\mathcal{L}}+\Gamma)\otimes I_u)\widehat{J}(\hat{\boldsymbol{a}}(t)))^{\mathrm{T}}\delta_1(t)\\ \quad+\mathcal{O}^{\mathrm{T}}(t)\delta_3(t)=\mathbf{0},\\ I_{k^2}\delta_2(t)=\mathbf{0},\\ ((\mathcal{H}\widetilde{\mathcal{L}}+\Gamma)\otimes I_u)(\widehat{J}(\hat{\boldsymbol{a}}(t))\dot{\hat{\boldsymbol{a}}}(t)+\widehat{\boldsymbol{\varpi}}(t))\\ \quad-\Gamma\otimes I_u\cdot\mathbf{1}_k\otimes(\dot{\boldsymbol{r}}_{\mathbf{d}}(t)+\boldsymbol{r}_{\mathbf{d}}(t))=\mathbf{0},\\ \dot{\boldsymbol{h}}(t)+(\widetilde{\mathcal{L}}\otimes I_k)\boldsymbol{h}(t)=\mathbf{0},\\ \aleph_{\text{NCP}}(\delta_3(t),\mathcal{O}(t)\dot{\hat{\boldsymbol{a}}}(t)-\mathcal{T}(t))=\mathbf{0}.\end{cases}$$

Combining the above equations, the distributed and weight-unbalanced collaborative control scheme (9) is transferred to

$$\Upsilon(t)\boldsymbol{f}(t)=\digamma(t),\tag{11}$$

where

$$\Upsilon(t)=\begin{bmatrix}I_{mk}&\mathbf{0}&\Upsilon_1^{\mathrm{T}}(t)&\mathbf{0}&\mathcal{O}^{\mathrm{T}}(t)\\ \mathbf{0}&\mathbf{0}&\mathbf{0}&I_{k^2}&\mathbf{0}\\ \Upsilon_1(t)/2\mathfrak{g}&\mathbf{0}&\mathbf{0}&\mathbf{0}&\mathbf{0}\\ \mathbf{0}&I_{k^2}&\mathbf{0}&\mathbf{0}&\mathbf{0}\\ \mathcal{O}(t)&\mathbf{0}&\mathbf{0}&\mathbf{0}&I_{2mk}\end{bmatrix},$$

$$\boldsymbol{f}(t)=\begin{bmatrix}2\mathfrak{g}\dot{\hat{\boldsymbol{a}}}(t)\\ \dot{\boldsymbol{h}}(t)\\ \delta_1(t)\\ \delta_2(t)\\ \delta_3(t)\end{bmatrix},\digamma(t)=\begin{bmatrix}-2\mathfrak{g}\boldsymbol{z}\\ \mathbf{0}\\ \digamma_1(t)\\ \digamma_2(t)\\ \digamma_3(t)\end{bmatrix},$$

in which $\Upsilon_1(t)=((\mathcal{H}\widetilde{\mathcal{L}}+\Gamma)\otimes I_u)\widehat{J}(\hat{\boldsymbol{a}}(t))$, $\digamma_1(t)=\Gamma\otimes I_u\cdot\mathbf{1}_k\otimes(\dot{\boldsymbol{r}}_{\mathbf{d}}(t)+\boldsymbol{r}_{\mathbf{d}}(t))-((\mathcal{H}\widetilde{\mathcal{L}}+\Gamma)\otimes I_u)\widehat{\boldsymbol{\varpi}}(t)$, $\digamma_2(t)=-(\widetilde{\mathcal{L}}\otimes I_k)\boldsymbol{h}(t)$, $\digamma_3(t)=\mathcal{T}(t)+\sqrt{\delta_3(t)\circ\delta_3(t)+\boldsymbol{y}(t)\circ\boldsymbol{y}(t)+\boldsymbol{\eta}}$ with $\boldsymbol{y}(t)=\mathcal{O}(t)\dot{\hat{\boldsymbol{a}}}(t)-\mathcal{T}(t)$. Then, we can define an error function $\mathsf{e}(t)$:

$$\mathsf{e}(t)=\Upsilon(t)\boldsymbol{f}(t)-\digamma(t)\in\mathbb{R}^{2k^2+3mk+uk}.\tag{12}$$

Then, the neural dynamics design formula $\dot{\mathsf{e}}(t)=-\varepsilon\mathsf{e}(t)$ with $\varepsilon>0$ is introduced to realize the convergence of $\mathsf{e}(t)$. As a result, a distributed and weight-unbalanced neural dynamics controller that describes the solution of the QP optimization problem (9) is built:

$$\Upsilon(t)\dot{\boldsymbol{f}}(t) = -\dot{\Upsilon}(t)\boldsymbol{f}(t) - \varepsilon(\Upsilon(t)\boldsymbol{f}(t) - \digamma(t)) + \dot{\digamma}(t). \quad (13)$$

B. Theoretical Analyses

In this part, theoretical analyses are conducted for the distributed and weight-unbalanced neural dynamics controller (13) with stability and convergence proved in Theorem 2.

Theorem 2: As $\varepsilon > 0$, the distributed and weight-unbalanced neural dynamics controller (13) is stable in the Lyapunov sense and is convergent exponentially to a global optimal point $\boldsymbol{f}^*$, which is the desired solution of the distributed and weight-unbalanced collaborative control scheme (9).

Proof: The stability of the distributed and weight-unbalanced neural dynamics controller (13) can be proved by designing a Lyapunov function $\boldsymbol{v}(t) = \mathrm{e}^2(t) > \mathbf{0}$. Then, we can use the neural dynamics design formula $\dot{\mathrm{e}}(t) = -\varepsilon\mathrm{e}(t)$ to compute its time derivative $\dot{\boldsymbol{v}}(t) = -2\varepsilon\mathrm{e}^2(t) < \mathbf{0}$. Therefore, according to the Lyapunov stability theorems, the proposed distributed and weight-unbalanced neural dynamics controller is stable.

Besides, the convergence proof of the proposed controller (13) is provided as follows.

First, we present an error function $\boldsymbol{e}(t)$ denoting the difference between the obtained solution $\boldsymbol{f}(t)$ and the optimal one $\boldsymbol{f}^*(t)$:

$$\boldsymbol{e}(t) = \boldsymbol{f}(t) - \boldsymbol{f}^*(t). \quad (14)$$

Then, substituting $\boldsymbol{f}(t)$, $\dot{\boldsymbol{f}}(t)$ by $\boldsymbol{e}(t)+\boldsymbol{f}^*(t)$ and $\dot{\boldsymbol{e}}(t)+\dot{\boldsymbol{f}}^*(t)$ in the proposed controller (13), respectively:

$$\begin{aligned}&\varepsilon\left[\Upsilon(t)(\boldsymbol{e}(t) + \boldsymbol{f}^*(t)) - \digamma(t)\right] = \quad (15)\\ &-\Upsilon(t)(\dot{\boldsymbol{e}}(t) + \dot{\boldsymbol{f}}^*(t)) - \dot{\Upsilon}(t)(\boldsymbol{e}(t) + \boldsymbol{f}^*(t)) + \dot{\digamma}(t).\end{aligned}$$

After reorganizing, we can obtain the following formula:

$$\begin{aligned}&\varepsilon\Upsilon(t)\boldsymbol{e}(t) + \varepsilon\Upsilon(t)\boldsymbol{f}^*(t) - \varepsilon\digamma(t) = \quad (16)\\ &-\Upsilon(t)\dot{\boldsymbol{e}}(t) - \Upsilon(t)\dot{\boldsymbol{f}}^*(t) - \dot{\Upsilon}(t)\boldsymbol{e}(t) - \dot{\Upsilon}(t)\boldsymbol{f}^*(t) + \dot{\digamma}(t).\end{aligned}$$

It can be found that $\boldsymbol{f}^*(t)$ satisfies $\Upsilon(t)\boldsymbol{f}^*(t) - \digamma(t) = 0$, as well as its time derivative $\dot{\Upsilon}(t)\boldsymbol{f}^*(t) + \Upsilon(t)\dot{\boldsymbol{f}}^*(t) - \dot{\digamma}(t) = 0$. To simplify (16), we can deduce an equation:

$$\varepsilon\Upsilon(t)\boldsymbol{e}(t) = -\Upsilon(t)\dot{\boldsymbol{e}}(t) - \dot{\Upsilon}(t)\boldsymbol{e}(t). \quad (17)$$

We can observe that equation (17) has the same form as the ordinary differential equation and can be converted to

$$\frac{\mathrm{d}\Theta}{\mathrm{d}t} + \varepsilon\Theta = \mathbf{0}, \quad (18)$$

where $\Theta = \Upsilon(t)\boldsymbol{e}(t)$. This kind of ordinary differential equation has a general solution $\Theta = \mathcal{C}e^{-\varepsilon t}$ with $\mathcal{C} \in \mathbb{R}$, which can be finally concluded that the proposed controller (13) is exponentially convergent.

In a nutshell, the proposed controller (13) is stable and convergent to a global optimal point $\boldsymbol{f}^*$. ■

IV. Experimental Simulations and Comparisons

In this part, related experimental examples and comparisons are implemented to illustrate that the proposed distributed and weight-unbalanced collaborative control scheme (9) and the distributed and weight-unbalanced neural dynamics controller (13) are both feasible.

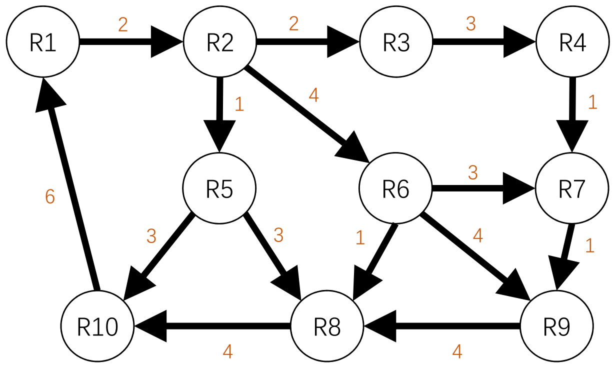

Fig. 2. Topology of the weight-unbalanced directed graph in these experiments.

A. Distributed Collaborative Control Under Weight-Unbalanced Directed Graphs

The proposed scheme (9) and its corresponding neural dynamics controller (13) mainly focus on the distributed collaborative control of MR^{2}S under weight-unbalanced directed graphs, so they can be applied in plenty of circumstances. For instance, in the automobile industry, multiple robots are utilized for coordinated welding [10], which can be seen as the collaborative control of MR^{2}S under weight-unbalanced directed graphs, and thus the proposed scheme and controller are available. This subsection offers a related experimental example.

UR5 is a redundant robot with six DOFs which is launched by the Universe Robots company. We consider ten UR5 robots as experimental devices for collaborative control. In MR^{2}S, moving an object together can be seen as one of the significant application scenarios of collaborative control, which requires the relative trajectories of all robots' end-effectors to stay consistent. The following experimental example simulates the above circumstance. These ten UR5 robots are set to complete an astroid line with the line equation $x(t) = 0.3\cos^5(t), y(t) = 0.3\sin^5(t)$. As for the distributed manner, it is ruled that only robot R1 and robot R5 can access the command center, i.e., $\Gamma(i,i) = 1$ when $i = 1, 5$, and the weight-unbalanced directed graph of robots is plotted in Fig. 2.

In this example, $\boldsymbol{z}$ in the objective function is designed as $\boldsymbol{z} = 10(\widehat{\boldsymbol{a}}(t) - \widehat{\boldsymbol{a}}(0))$, $\widehat{\boldsymbol{a}}(0) = [\boldsymbol{a}_1^{\mathrm{T}}(0), \cdots, \boldsymbol{a}_k^{\mathrm{T}}(0)]^{\mathrm{T}} \in \mathbb{R}^{mk}$ with $\boldsymbol{a}_i(0)$ representing robot i's initial joint angles. The values of parameters defined above are stipulated as $\dot{\widehat{\boldsymbol{a}}}_{\mathrm{L}}^{\mathrm{T}} = -2 * \mathbf{1}_{6k}$ rad/s, $\dot{\widehat{\boldsymbol{a}}}_{\mathrm{U}}^{\mathrm{T}} = 2.1 * \mathbf{1}_{6k}$ rad/s, $\mathfrak{g} = 0.5$, $\varepsilon = 10$, the number of UR5 robots $k = 10$, the experimental example duration $T = 2\pi$ s. The Laplacian matrix $\widetilde{\mathcal{L}}$ of the weight-unbalanced directed graph in this example is calculated as

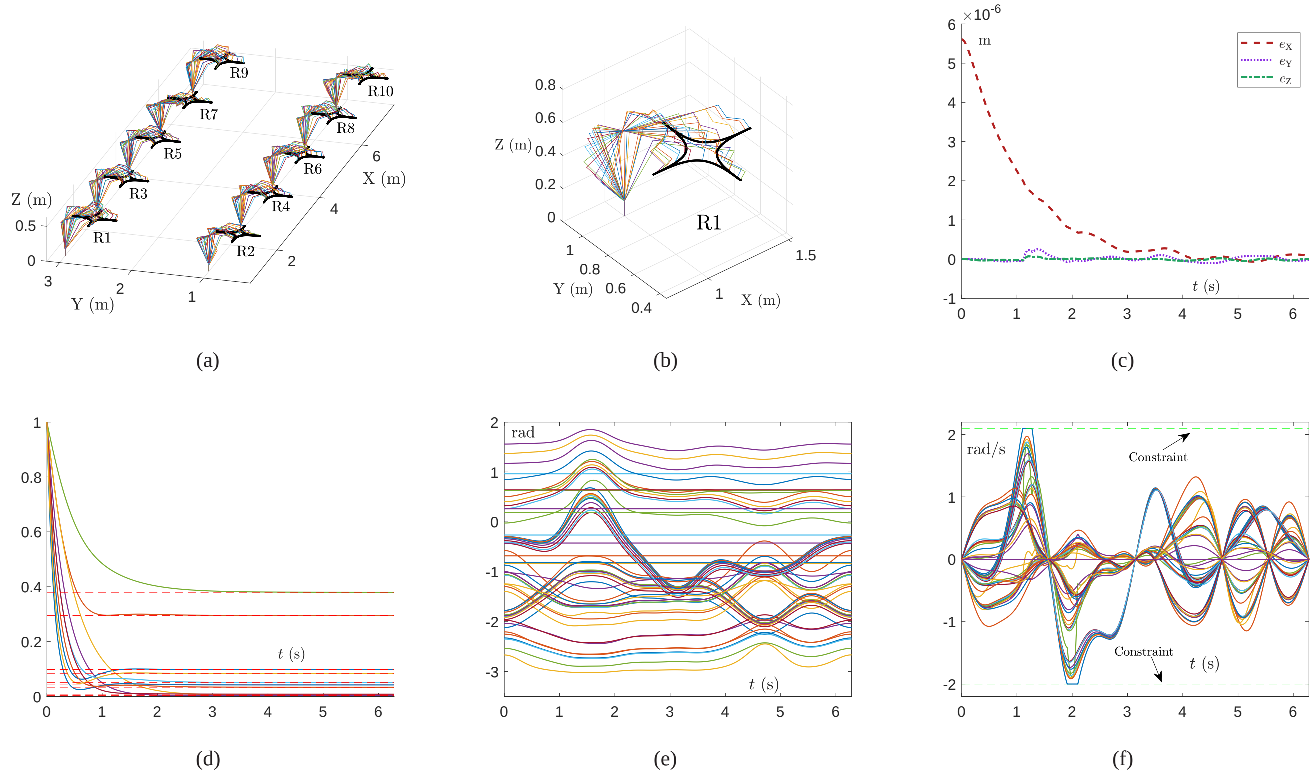

Fig. 3. Experimental example conducted by applying the distributed and weight-unbalanced collaborative control scheme (9) and the corresponding neural dynamics controller (13) for the collaborative control of ten UR5 robots to track a desired astroid line. (a) 3-D graph of ten UR5 robots in the whole process. (b) Detailed attitude of robot R1 from the beginning to the end. (c) Position errors of end-effectors. (d) Tendency of diagonal elements of $\mathcal{H}$. (e) Joint angles. (f) Joint velocities with a constraint.

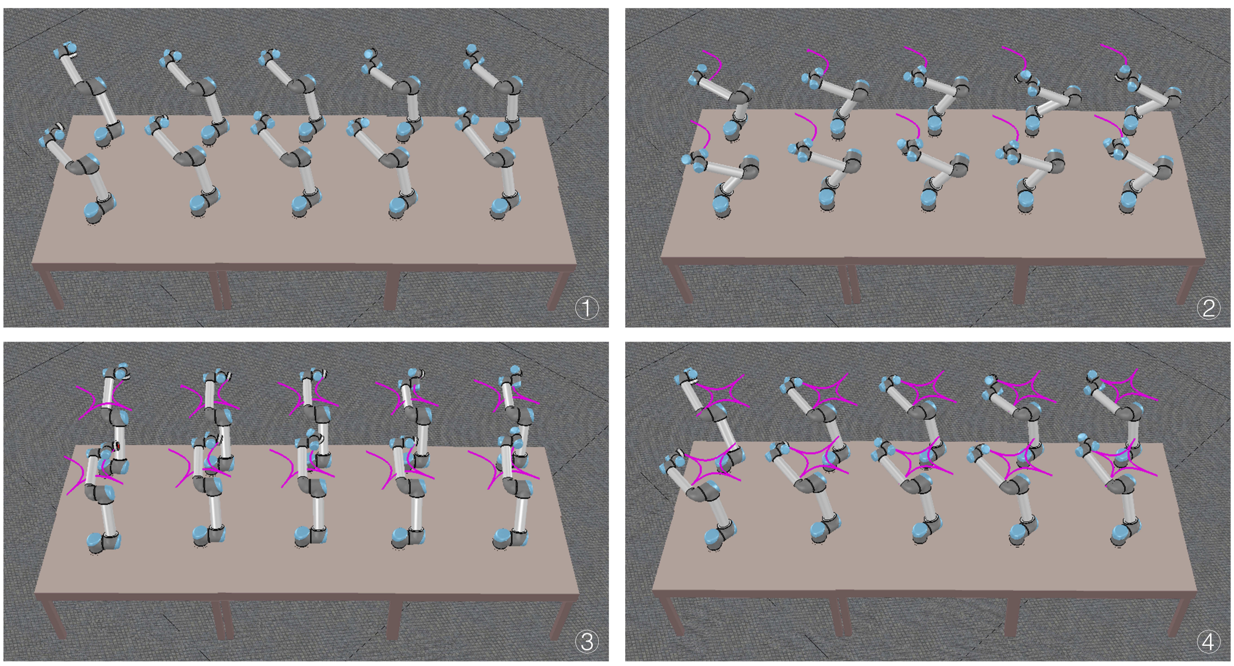

Fig. 4. Four experiment snapshots of ten UR5 robots on Coppeliasim applying the proposed distributed and weight-unbalanced neural dynamics controller (13) to execute an astroid line.

TABLE II
COMPARISONS OF THE CONTROL SCHEMES OF REDUNDANT ROBOTS AMONG DIFFERENT PAPERS

	Weight-Unbalanced Directed Graph Considered	Robots Numbers	Topology Type	Limited Communication	Performance Index	Problem Formulation
Scheme (9) in this paper	Yes	Multiple	Distributed	Yes	GPI$^\sharp$	Optimization
Scheme in [9]	No	Single	N/A§	N/A§	CMG$^\circlearrowleft$	Optimization
Scheme in [12]	No	Two	Decentralized	No	N/A§	Adaptive Control
Scheme in [13]	No	Multiple	Decentralized	No	MVN$^\natural$	Optimization
Scheme in [14]	No	Multiple	Distributed	Yes	Manipulability	Optimization
Scheme in [24]	No	Multiple	Distributed	Yes	MVN$^\natural$	Game-Theoretic
Scheme in [25]	No	Multiple	Distributed	Yes	RMP$^\heartsuit$	Optimization
Scheme in [29]	Yes	N/A§	Distributed	N/A§	N/A§	Graph Theory

$^\sharp$: GPI is a shortened form of generalized performance index.
§: N/A denotes that the comparing item is not practicable in that article.
$^\circlearrowleft$: CMG is a shortened form of cyclic motion generation.
$^\natural$: MVN is a shortened form of minimum velocity norm.
$^\heartsuit$: RMP is a shortened form of repetitive motion planning.

follows:

$$\widetilde{\mathcal{L}}=\begin{bmatrix} 6 & 0 & 0 & 0 & 0 & 0 & 0 & 0 & 0 & -6 \\ -2 & 2 & 0 & 0 & 0 & 0 & 0 & 0 & 0 & 0 \\ 0 & -2 & 2 & 0 & 0 & 0 & 0 & 0 & 0 & 0 \\ 0 & 0 & -3 & 3 & 0 & 0 & 0 & 0 & 0 & 0 \\ 0 & -1 & 0 & 0 & 1 & 0 & -1 & 0 & 0 & 0 \\ 0 & -4 & 0 & 0 & 0 & 4 & 0 & 0 & 0 & 0 \\ 0 & 0 & 0 & -1 & 0 & -3 & 4 & 0 & -1 & 0 \\ 0 & 0 & 0 & 0 & -3 & -1 & 0 & 8 & -4 & 0 \\ 0 & 0 & 0 & 0 & 0 & -4 & -1 & 0 & 5 & -1 \\ 0 & 0 & 0 & 0 & -3 & 0 & 0 & -4 & 0 & 7 \end{bmatrix}.$$

Besides, assigning the rest parameters to zero. Then, the experimental results are illustrated in Fig. 3.

It can be seen that six subfigures are shown in Fig. 3. Figure 3(a) shows the 3-D graph of all joints of ten UR5 robots in a whole experimental process with black lines denoting the end-effector trajectories. We can notice that different redundant robots have different poses to conduct a same given task. What is more, it can be seen that Fig. 3(b) illustrates the detailed attitude of robot R1 from the beginning to the end, from which we can see that the entire motion of robot R1 is very smooth. Besides, the colorful lines instead of the black line in Fig. 3(a) and Fig. 3(b) represent the whole three-dimensional posture of robots at various historical moments. The end-effector position errors are depicted in Fig. 3(c), from which we can see that the position errors are all of the order 10^{-6} m, so the proposed scheme and the corresponding controller possess satisfying accuracy. Figure 3(d) provides the tendency of diagonal elements of $\mathcal{H}$, where the red dashed lines represent the calculated left eigenvector $\boldsymbol{q}^{\mathrm{T}}$ = [0.0985, 0.2954, 0.0042, 0.0028, 0.3797, 0.0506, 0.0084, 0.0422, 0.0338, 0.0844] of $\widetilde{\mathcal{L}}$ with eigenvalue being 0. It can be seen that all the diagonal elements of $\mathcal{H}$ converge to red dashed lines no more than 4 s, which means that our proposed scheme can estimate $\boldsymbol{q}^{\mathrm{T}}$ effectively, thus available for handling circumstances under weight-unbalanced directed graphs. Joint angles of ten UR5 robots are plotted in Fig. 3(e). As we can see, the initial joint angles $\widehat{\boldsymbol{a}}(0)$ of UR5 robots are discrepant, and the final states equal $\widehat{\boldsymbol{a}}(0)$ intuitively, which means that these UR5 robots possess the property of redundancy as they can not only conduct a given mission but also satisfy the defined generalized performance index. In Fig. 3(f), joint velocities of ten UR5 robots in the experiment duration are displayed, and it can be found that joint velocities are constrained in a required scope, which demonstrates the feasibility of the inequality constraint. In a nutshell, the above results prove the feasibility of the proposed distributed and weight-unbalanced collaborative control scheme (9) and its corresponding neural dynamics controller(13).

In order to demonstrate the correctness of (13), we conduct an experiment on CoppeliaSim by placing ten UR5 robots to track the astroid line. CoppeliaSim is a common-used tool with a large number of devices, such as desks and redundant robots. All the parameters in this experiment are identical to those before. In Fig. 4, four experiment snapshots of ten UR5 robots on Coppeliasim applying the proposed distributed and weight-unbalanced neural dynamics controller (13) are shown to execute an astroid line successfully. This experiment intuitively manifests that (13) is applicable and feasible.

B. Comparisons

This subsection makes some comparisons on related items about the control of MR^{2}S among the proposed scheme (13) and other schemes presented in [9], [12]–[14], [24], [25], [29], respectively. In detail, a scheme with its performance index being cyclic motion generation is presented in [9] for the control of a single redundant robot. As for [12], the decentralized cooperative control scheme of two robots is investigated with the help of adaptive control. In [14], the manipulability of multiple mobile robots is optimized for their distributed cooperative transportation control. Besides, schemes in [24], [25] are mainly devoted to the distributed control of MR^{2}S with different emphases, such as communication efficiency and the game-theoretical perspective [24], time delays [25]. Additionally, the distributed average tracking problems under weight-unbalanced directed graphs in a particle level in multi-agent systems are investigated in [29] by presenting two algorithms. It can be clearly seen that weight-unbalanced directed graphs are firstly taken into account in the proposed scheme (9) in this paper for the distributed collaborative control of MR^{2}S with robots kinematics and strict theorems on the stability and convergence contained. Besides, our proposed method (9) adopts a generalized performance index to increase the scalability and a joint velocity constraint to protect the robot. Table II is intuitively tabulated with the above discussions and comparisons included.

V. Conclusions

A distributed and weight-unbalanced neural dynamics scheme for the collaborative control in multiple redundant robot systems (MR^2S) has been proposed in this paper. The proposed scheme merges weight-unbalanced directed graphs in the collaborative control of MR^2S with robot kinematics contained for the first time, and the required left eigenvector has been estimated satisfyingly to ensure that the scheme is stable and convergent. Besides, constraint on the joint velocities and generalized performance index are designed for increasing the safety and scalability of the proposed scheme. Then, a neural dynamics controller has been designed to solve the above problems with theoretical proofs provided to substantiate its feasibility. Additionally, the results of experimental examples and comparisons have proved the validity of the proposed scheme and controller. Furthermore, the collaborative control of MR^2S with switching topology is one of the significant directions in the future.

References

[1] E. Dean-Leon, K. Ramirez-Amaro, F. Bergner, I. Dianov, and G. Cheng, "Integration of robotic technologies for rapidly deployable robots," *IEEE Trans. Ind. Informat.*, vol. 14, no. 4, pp. 1691–1700, Apr. 2018.

[2] Z. Nie and K. -C. Chen, "Hypergraphical real-time multi-robot task allocation in a smart factory," *IEEE Trans. Ind. Informat.*, vol. 18, no. 9, pp. 6047–6056, Sept. 2022.

[3] B. Wu, J. Zhong, and C. Yang, "A visual-based gesture prediction framework applied in social robots," *IEEE/CAA J. Autom. Sinica*, vol. 9, no. 3, pp. 510–519, Mar. 2022.

[4] Z. Peng, J. Wang, and Q. -L. Han, "Path-following control of autonomous underwater vehicles subject to velocity and input constraints via neurodynamic optimization," *IEEE Trans. Ind. Electron.*, vol. 66, no. 11, pp. 8724–8732, Nov. 2019.

[5] Z. Li and S. Li, "Recursive recurrent neural network: A novel model for manipulator control with different levels of physical constraints," *CAAI Trans. Intell. Technol.*, to be published. DOI: 10.1049/cit2.12125.

[6] H. Zhang, H. Jin, Z. Liu, Y. Liu, Y. Zhu, and J. Zhao, "Real-time kinematic control for redundant manipulators in a time-varying environment: Multiple-dynamic obstacle avoidance and fast tracking of a moving object," *IEEE Trans. Ind. Informat.*, vol. 16, no. 1, pp. 28–41, Jan. 2020.

[7] B. Liao and W. Liu, "Pseudoinverse-type bi-criteria minimization scheme for redundancy resolution of robot manipulators," *Robotica*, vol. 33, no. 10, pp. 2100–2113, May 2014.

[8] J. S. Wang, J. Wang, and Q. -L. Han, "Neurodynamics-based model predictive control of continuous-time under-actuated mechatronic systems," *IEEE/ASME Trans. Mechatron.*, vol. 26, no. 1, pp. 311–322, Feb. 2021.

[9] Z. Xie, L. Jin, X. Luo, S. Li, and X. Xiao, "A data-driven cyclic-motion generation scheme for kinematic control of redundant manipulators," *IEEE Trans. Control Syst. Technol.*, vol. 29, no. 1, pp. 53–63, Jan. 2021.

[10] Q. Wang, W. Jiao, P. Wang, and Y. Zhang, "Digital twin for human-robot interactive welding and welder behavior analysis," *IEEE/CAA J. Autom. Sinica*, vol. 8, no. 2, pp. 334–343, Nov. 2020.

[11] Y. He, Z. Deng, and J. Zhang, "Design and voice-based control of a nasal endoscopic surgical robot," *CAAI Trans. Intell. Technol.*, vol. 6, pp. 123–131, Mar. 2021.

[12] W. Gueaieb, F. Karray, and S. Al-Sharhan, "A robust hybrid intelligent position/force control scheme for cooperative manipulators," *IEEE/ASME Trans. Mechatronics*, vol. 12, no. 2, pp. 109–125, Apr. 2007.

[13] S. Li, S. Chen, B. Liu, Y. Li, and Y. Liang, "Decentralized kinematic control of a class of collaborative redundant manipulators via recurrent neural networks," *Neurocomputing*, vol. 91, pp. 1–10, Aug. 2012.

[14] J. Chen and S. Kai, "Cooperative transportation control of multiple mobile manipulators through distributed optimization," *Inform. Sciences*, vol. 61, no. 12, pp. 1–17, Dec. 2018.

[15] X. Ge, Q. -L. Han, J. Wang, and X. -M. Zhang, "Scalable and resilient platooning control of cooperative automated vehicles," *IEEE Trans. Veh. Technol.*, vol. 71, no. 4, pp. 3595–3608, Apr. 2022.

[16] R. S. Sharma, A. Mondal, and L. Beher, "Tracking control of mobile robots in formation in the presence of disturbances," *IEEE Trans. Ind. Informat.*, vol. 17, no. 1, pp. 110–123, Jan. 2021.

[17] L. Kong, W. He, C. Yang, Z. Li, and C. Sun, "Adaptive fuzzy control for coordinated multiple robots with constraint using impedance learning," *IEEE Trans. Cybern*, vol. 49, no. 8, pp. 3052–3063, Aug. 2019.

[18] Z. Peng, J. Wang, D. Wang, and Q. -L. Han, "An overview of recent advances in coordinated control of multiple autonomous surface vehicles," *IEEE Trans. Ind. Informat.*, vol. 17, no. 2, pp. 732–745, Feb. 2021.

[19] J. Xu, X. He, X. Han, and H. Wen, "A two-layer distributed algorithm using neurodynamic system for solving L_1-minimization," *IEEE Trans. Circuits Syst. II, Exp. Briefs*, vol. 69, no. 8, pp. 3490–3494, Aug. 2022.

[20] Y. Zhang, S. S. Ge, and T. H. Lee, "Real-time kinematic control for redundant manipulators in a time-varying environment: Multiple-dynamic obstacle avoidance and fast tracking of a moving object," *IEEE Trans. Ind. Informat.*, vol. 16, no. 1, pp. 28–41, Jan. 2020.

[21] Z. Zhang, X. Deng, X. Qu, B. Liao, L. -D. Kong, and L. Li, "A varying-gain recurrent neural network and its application to solving online time-varying matrix equation," *IEEE Access*, vol. 6, pp. 77940–77952, Dec. 2018.

[22] Z. Tan, Y. Hu, L. Xiao, and K. Chen, "Robustness analysis and robotic application of combined function activated RNN for time-varying matrix pseudo inversion," *IEEE Access*, vol. 7, pp. 33434–33440, Mar. 2019.

[23] Y. Saad and H. A. van der Vorst, "Iterative solution of linear systems in the 20th century," *J. Computational Appl. Math.*, vol. 123, no. 1–2, pp. 1–33, Nov. 2000.

[24] J. Zhang, L. Jin, and C. Yang, "Distributed cooperative kinematic control of multiple robotic manipulators with improved communication efficiency," *IEEE/ASME Trans. Mechatron.*, vol. 27, no. 1, pp. 149–158, Feb. 2022.

[25] L. Jin, X. Zheng, and X. Luo, "Neural dynamics for distributed collaborative control of manipulators with time delays," *IEEE/CAA J. Autom. Sinica*, vol. 9, no. 5, pp. 854–863, May 2022.

[26] *Russian Su-57 stealth fighters deployed to suppress Ukrainian air defences – Reports*, Military Watch Magazine, Jun. 15, 2022. [Online]. Available: https://militarywatchmagazine.com/article/russian-su57-suppress-ukrainian-air-defence

[27] Y. Zhu, W. Yu, G. Wen, and W. Ren, "Continuous-time coordination algorithm for distributed convex optimization over weight-unbalanced directed networks," *IEEE Trans. Circuits Syst. II: Express Briefs*, vol. 66, no. 7, pp. 1202–1206, Jul. 2019.

[28] D. Wang, J. Yin, and W. Wang, "Distributed randomized gradient-free optimization protocol of multiagent systems over weight-unbalanced digraphs," *IEEE Trans. Cybern.*, vol. 51, no. 1, pp. 473–482, Jan. 2021.

[29] S. Sun, F. Chen, and W. Ren, "Distributed average tracking in weight-unbalanced directed networks," *IEEE Trans. Autom. Control*, vol. 66, no. 9, pp. 4436–4443, Sept. 2021.

[30] J. Zhang, L. Liu, H. Ji, and X. Wang, "Optimal output consensus of heterogeneous linear multiagent systems over weight-unbalanced directed networks," *IEEE Trans. Cybern.*, to be published. DOI: 10.1109/TCYB.2022.3191938.

[31] R. Olfati-Saber and R. M. Murray, "Consensus problems in networks of agents with switching topology and time-delays," *IEEE Trans. Autom. Control*, vol. 49, no. 9, pp. 1520–1533, Sept. 2004.

[32] Z. Li, Z. Ding, J. Sun, and Z. Li, "Distributed adaptive convex optimization on directed graphs via continuous-time algorithms," *IEEE Trans. Autom. Control*, vol. 63, no. 5, pp. 1434–1441, May 2018.

[33] Y. Lou, Y. Hong, L. Xie, G. Shi, and K. H. Johansson, "Nash equilibrium computation in subnetwork zero-sum games with switching communications," *IEEE Trans. Autom. Control*, vol. 61, no. 10, pp. 2930–2935, Oct. 2016.

[34] S. Boyd and L. Vandenberghe, *Convex Optimization*. Cambridge U.K.: Cambridge Univ. Press, 2004.

[35] X. Huang, X. Lou, and B. Cui, "A novel neural network for solving convex quadratic programming problems subject to equality and inequality constraints," *Neurocomputing*, vol. 214, pp. 23–31, Nov. 2016.

Xin Zheng received the B.E. degree in communication engineering from Lanzhou University, Lanzhou, China, in 2020, and he is currently pursuing the M.E. degree in information and communication engineering with the School of Information Science and Engineering in Lanzhou University.

His current research interests include multi-robot collaboration and neural dynamics.

Mei Liu received the B.E. degree in communication engineering from Yantai University, Yantai, China, in 2011, and the M.E. degree in pattern recognition and intelligent system from Sun Yat-sen University, Guangzhou, China, in 2014. After that, she joined Jishou University as a lecturer. From 2016 to 2017, she had been with the Department of Computing, the Hong Kong Polytechnic University as a Research Assistant. Currently, she conducts studies and research with Lanzhou University, Lanzhou, China, and University of Chinese Academy of Sciences, Beijing, China. Her main research interests include neural networks, robotics and optimization.

Long Jin (Senior Member, IEEE) received the B.E. degree and the Ph.D. degree from Sun Yat-sen University, Guangzhou, China, in 2011 and 2016, respectively. He received postdoctoral training at the Department of Computing, The Hong Kong Polytechnic University, Hong Kong, from 2016 to 2017. In 2017, he joined the School of Information Science and Engineering, Lanzhou University, as a Professor of computer science and engineering. He received the Outstanding Ph.D. Dissertation Award in 2018 and the Wu Wen-Jun Artificial Intelligence Excellent Youth in 2021, both from Chinese Association for Artificial Intelligence (CAAI). His current research interests include neural networks, robotics, optimization, and intelligent computing.

Chenguang Yang (Senior Member, IEEE) received the Ph.D. degree in control engineering from the National University of Singapore, Singapore, in 2010, and postdoctoral training in human robotics from the Imperial College London, London, U.K. He was awarded UK EPSRC UKRI Innovation Fellowship and individual EU Marie Curie International Incoming Fellowship. As the lead author, he won the IEEE Transactions on Robotics Best Paper Award (2012) and IEEE Transactions on Neural Networks and Learning Systems Outstanding Paper Award (2022). He is the Corresponding Co-Chair of IEEE Technical Committee on Collaborative Automation for Flexible Manufacturing, a Fellow of Institute of Engineering and Technology (IET), a Fellow of Institution of Mechanical Engineers (IMechE), and a Fellow of British Computer Society (BCS). His research interest lies in human robot interaction and intelligent system design.